IEEE Access
Multidisciplinary ⋮ Rapid Review ⋮ Open Access Journal

Received 6 March 2023, accepted 24 March 2023, date of publication 27 March 2023, date of current version 30 March 2023.

Digital Object Identifier 10.1109/ACCESS.2023.3262295

RESEARCH ARTICLE

Design of Compact Self-Quintuplexing Antenna With High-Isolation for Penta-Band Applications

RUSAN KUMAR BARIK[1], (Member, IEEE), AND SLAWOMIR KOZIEL[1,2], (Fellow, IEEE)
[1]Department of Engineering, Reykjavik University, 102 Reykjavik, Iceland
[2]Faculty of Electronics, Telecommunications and Informatics, Gdańsk University of Technology, 80-233 Gdansk, Poland

Corresponding author: Slawomir Koziel (koziel@ru.is)

This work was supported in part by the Icelandic Centre for Research (RANNIS) under Grant 217771, and in part by the National Science Centre of Poland under Grant 2020/37/B/ST7/01448.

ABSTRACT This article presents a novel compact self-quintuplexing antenna architecture based on a substrate-integrated rectangular cavity (SIRC) for pentaband applications. The proposed self-quintuplexing antenna is constructed by employing an SIRC, one Pi-shaped slot (PSS), one T-shaped slot (TSS), and five 50Ω microstrip feedlines. The PSS and TSS are engraved on the top of the SIRC to create five radiating patches, which are excited by five 50Ω feedlines to achieve pentaband operation with self-quintuplexing characteristics. The resonating frequencies can be tuned independently based on the dimension of the radiator without disturbing other bands. A detailed parametric analysis is carried out to provide a suitable frequency tunable range and high isolation. In addition, an equivalent lumped circuit is developed to analyze the proposed self-quintuplexing antenna. To validate the proposed antenna architecture, an SIRC-based self-quintuplexing antenna operating at 2.29, 2.98, 3.65, 4.37, and 5.08 GHz is fabricated and demonstrated. The fabricated antenna offers competitive performance with a compact size of $0.173\lambda^2$, pentaband operation, high isolation of 29.31 dB, and a wide frequency tunability range from 2.29 GHz to 6.03 GHz. Furthermore, the fabricated self-quintuplexing antenna exhibits the measured realized gain of 3.59, 4.55, 3.91, 5.70, and 4.92dBi at 2.29, 2.98, 3.64, 4.37, and 5.08 GHz, respectively.

INDEX TERMS Substrate-integrated rectangular cavity, self-quintuplexing, antenna, pentaband.

I. INTRODUCTION

The ever-increasing demand for multi-standard systems and the rapid revolution of next-generation wireless technologies have made antenna design more challenging. To accommodate multiple standards into a single system, multiple planar antennas are required, which not only increases the size of the wireless system but also leads to interference between the antennas. To mitigate this issue, the best solution for multi-standard applications is a single-feed antenna with multiple resonances supporting various bands and effortlessly adapting to the shape of new communication systems due to their lightweight, small footprint, low cost, and easy manufacturing [1], [2], [3], [4], [5], [6], [7]. In the literature, several design techniques have been demonstrated for quad-band operations [1], [2], [3], pentaband operations [4], [5], [6], and hexa-band operations [7]. However, these architectures require external multiplexer circuits to select the frequency bands and need more space to be accommodated in the system. In light of these issues, new types of antenna architectures have been constructed to allow multi-band operation with inherent multiplexing characteristics. For such structures, external multiplexer circuits are not required for operating band selection.

Over the last few years, substrate-integrated waveguide (SIW)-based antennas have received a lot of attention due to their small size, multi-band operation, superior isolation, and enhanced radiation properties [8], [9]. Recently, many self-diplexing antennas [10], [11], [12], [13], [14], self-triplexing antennas [15], [16], [17], [18], self-quadruplexing antennas [19], [20], [21], [22], [23], [24], and self-multiplexing antennas for hexaband applications [25], [26] have been

The associate editor coordinating the review of this manuscript and approving it for publication was Debabrata K. Karmokar.

reported. Generally, two, three, four, and six feeding ports are applied to develop self-diplexing, self-triplexing, self-quadruplexing, and self-multiplexing antennas that radiate at dual, triple, quad, and hexa operating bands, respectively. A cavity-backed bowtie-ring slot [10], a U-shaped slot [11], a shielded SIW cavity-backed Y-shaped slot [12] and two U-shaped slots [13], and two coaxial feed-modified half-mode SIW (HMSIW) cavity [14] have been demonstrated for the self-diplexing antennas (SDAs). Self-triplexing antennas (STAs) have been constructed by employing SIW square cavity-backed modified I-shaped slot [15], HMSIW cavity-backed V-shaped slots [16], and hexagonal SIW loaded with rectangular cavities [17].

Recently, several self-quadruplexing antennas have been designed using a number of new SIW cavity-backed slot resonators [18], [19], [20], [21], [22], [23], [24]. In [18], self-quadruplexing antennas with circular polarization characteristics have been implemented using a square SIW cavity with T-shaped slots. In [19], the synthesis of a self-quadruplexing antenna has been introduced by using four quarter-mode SIW cavities with V-shaped slots. In [20], the square SIW cavity's top surface has been altered to create patches of varying widths that radiate at four different frequencies. Four unequal quarter-mode SIW (QMSIW) cavities have been used to construct a self-quadruplexing antenna [21]. Four unequal QMSIW resonators have been produced by dividing a full-mode circular SIW cavity to realize a self-quadruplexing antenna [22]. In [23], a self-quadruplexing slot antenna for microwave and mm-wave applications has been built using half-mode SIW cavity resonators. In [24], two U-shaped slots have been loaded on the cavity to realize a self-quadruplexing antenna. In [25] and [26], self-multiplexing antennas (SMA) have been constructed by producing rectangular patches on top of a SIW cavity for hexa-band applications. Although the aforementioned self-multiplexing antenna structures have competitive performance, it is still challenging to construct a self-quintuplexing antenna that is compact yet exhibits high isolation and pentaband operation.

This communication presents a novel self-quintuplexing antenna (SQA) configuration for pentaband applications. The proposed SQA is realized by employing a substrate-integrated rectangular cavity (SIRC) resonator, a Pi-shaped slot (PSS), and a T-shaped slot (TSS). The self-quintuplexing antenna is excited by five microstrip inset feedlines to allow radiation at 2.29, 2.98, 3.65, 4.37, and 5.08 GHz. The proposed SQA delivers high isolation, compact size, flexible frequency re-designability, and good radiation characteristics. For validation, a prototype of SQA is fabricated and demonstrated. The main contributions of the suggested SQA can be summarized as follows:

1) To the best of the author's knowledge, the self-quintuplexing antenna for pentaband operation is presented for the first time in the literature;

2) The proposed SQA configuration occupies a smaller footprint area of $0.173\lambda^2$, which is smaller than the existing self-quadruplexing/multiplexing antennas in the literature;

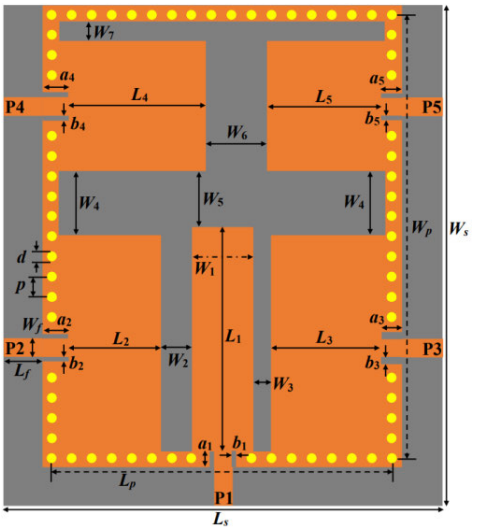

FIGURE 1. Configuration of the proposed SIRC-based self-quintuplexing antenna. The design parameter values are: $L_s = 44$, $W_s = 52$, $L_p = 34$, $W_p = 42$, $L_f = 5.0$, $W_f = 2.16$, $L_1 = 19.8189$, $L_2 = 7.7936$, $L_3 = 10.6035$, $L_4 = 13.646$, $L_5 = 11.1176$, $W_1 = 5.9159$, $W_2 = 3.9397$, $W_3 = 1.5901$, $W_4 = 7.0$, $W_5 = 6.0$, $W_6 = 5.8653$, $W_7 = 2.0$, $a_1 = 1.9311$, $b_1 = 0.5526$, $a_2 = 3.3087$, $b_2 = 0.5747$, $a_3 = 2.8484$, $b_3 = 0.9387$, $a_4 = 2.8540$, $b_4 = 0.5378$, $a_5 = 2.5171$, $b_5 = 0.5001$, $d = 1.0$, $p = 2.0$; unit: mm.

3) Our SQA offers high isolation of greater than 29.31dB;

4) An equivalent circuit model is developed to validate the design;

5) The operating bands are re-designable in the range from 2.29 GHz to 6.03 GHz, which would accommodate several communications standards.

II. DESIGN PROCEDURE

Figure 1 shows the configuration of the proposed self-quintuplexing antenna (SQA) based on a substrate-integrated rectangular cavity (SIRC) resonator. The SQA is constructed using an SIRC resonator, one Pi-shaped slot (PSS), one T-shaped slot (TSS), and five 50 Ω microstrip feedlines. The PSS and TSS are engraved on the top of the SIRC resonator to create five patch radiators (PRs), which are excited by the microstrip inset feedlines to obtain the pentaband operation with self-quintuplexing properties. The structure is designed to achieve compact size, high isolation, wide frequency designability, and good radiation characteristics. Initially, an SIRC resonator ($L_p \times W_p$) is constructed on an Arlon AD250 substrate ($h_s = 0.762$mm, $\varepsilon_r = 2.5$, and $\tan\delta = 0.0014$). The EM simulation is carried out by CST Microwave Studio. The SIRC resonator is excited at the TE_{110} (fundamental mode), TE_{120}, and TE_{210} modes. The mode frequencies of the SIRC are determined as [5]:

$$f_{mn0}^{SIRC} = \frac{1}{2\pi\sqrt{\varepsilon_r}}\sqrt{\left(\frac{m\pi}{W_{eq}^{SIRC}}\right)^2 + \left(\frac{n\pi}{L_{eq}^{SIRC}}\right)^2} \quad (1)$$

where

$$\begin{cases} L_{eq}^{SIRC} = L_p - 1.08\frac{d^2}{p} + 0.1\frac{d^2}{L_p} \\ W_{eq}^{SIRC} = W_p - 1.08\frac{d^2}{p} + 0.1\frac{d^2}{W_p} \end{cases}$$

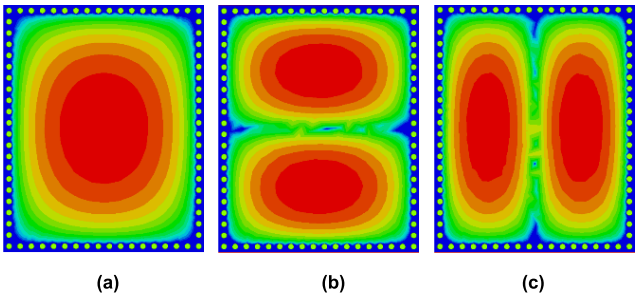

FIGURE 2. E-field distributions of full-mode SIRC resonator: (a) TE_{110} mode, (b) TE_{210} mode, and (c) TE_{120} mode.

The mode characteristics of the proposed SIRC are obtained by employing the eigenmode analysis. Figure 2 shows the electric field distributions for the resonating modes TE_{110}, TE_{120}, and TE_{210} excited at 3.64, 5.38, and 6.11 GHz, respectively. The unloaded quality factors Q_u for TE_{110}, TE_{120}, and TE_{210} modes are determined as 329, 362, and 371, respectively. Next, a PSS and TSS are superimposed on the top of the SIRC to produce five patch radiators (PRs). These PRs are excited by employing independent inset feedlines to enable radiation at five distinct operating bands. The surface current distribution at five operating frequencies on the antenna's top surface can be used to understand the radiation mechanism. Figure 3 shows the surface current distribution at individual ports causing radiation. The current distribution is obtained by exciting the PRs at one port and terminating other ports and vice versa. It is discovered that the surface current at individual ports is primarily focused on the excited radiating areas, with little current flowing into the remaining ports. Thus, it can be said that self-multiplexing is implemented and the isolations are improved.

The design parameters of the PSS and TSS play a significant role in obtaining compact size, high isolation, and wide frequency tunability. To achieve the good matching, the inline feed technique is applied at each port. The operating bands can be adjusted by appropriate tuning of the design parameters of PSS and TSS. Further, the transmission coefficients can be controlled by the parameters of the PSS. A comprehensive study of frequency tunability and isolation variation, along with an equivalent circuit model of the proposed SQA, will be discussed in the following subsections.

A. EQUIVALENT CIRCUIT MODEL

To validate the proposed self-quintuplexing antenna configuration, an equivalent circuit model is developed as shown in Fig. 4. The PSS and TSS are employed on the top of the SIRC to create five PRs, and each PR is represented by a parallel RLC network [8], [9], [10]. The resistances, capacitances, and inductances are denoted as R_{ai}, C_{ai}, and L_{ai}, respectively, where $i = 1, \ldots,$ and 5 stand for the respective port indices. The extra capacitances are generated due to the PSS and TSS, which are connected in shunt to the RLC circuit for each port. These capacitances are represented as C_{p1}, C_{p2}, C_{p3}, C_{p4}, and C_{p5} associated with ports 1 through 5, respectively. The

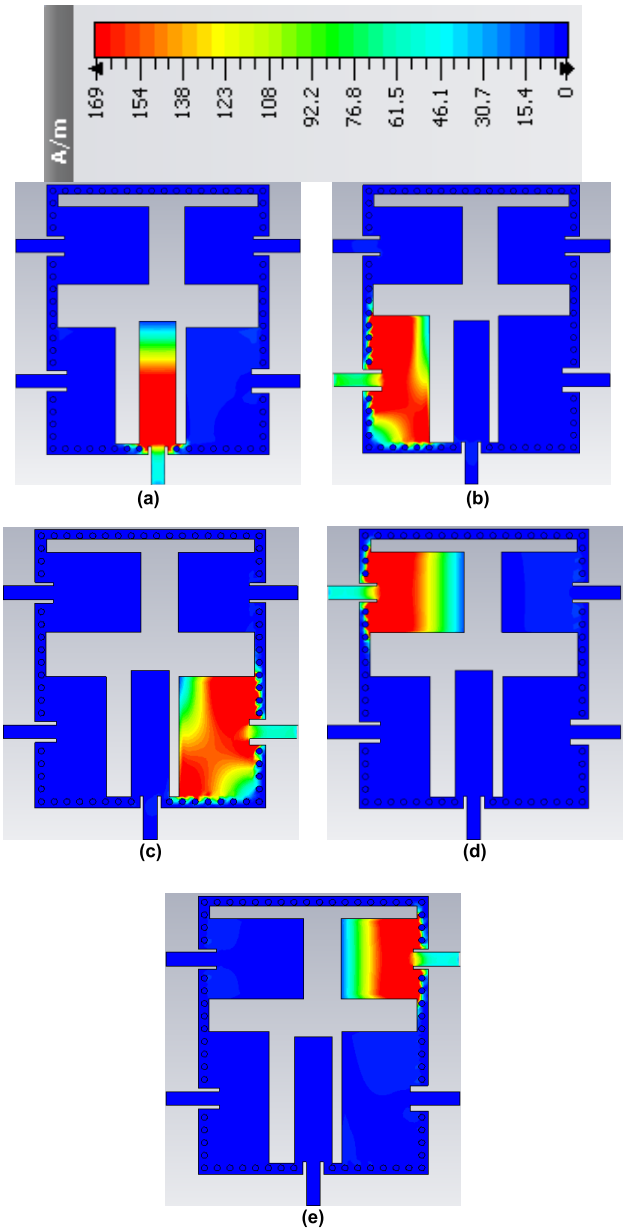

FIGURE 3. EM simulated surface current distributions on the top plane at different port excitation: (a) 2.29 GHz (port 1), (b) 5.08 GHz (port 2), (c) 4.37 GHz (port 3), (d) 2.98 GHz (port 4), and (e) 3.65 GHz (port 5).

couplings between the ports are expressed as M_{12}, M_{13}, M_{14}, M_{15}, M_{23}, M_{24}, M_{25}, M_{34}, M_{35}, and M_{45}. As can be seen in Fig. 5, series-connected LC circuit models each mutual coupling. The transformers express the matching between the ports and the RLC networks. The transformers T_1, T_2, T_3, T_4, and T_5 are used at port 1, port 2, port 3, port 4, and port 5, respectively. The operating frequencies and input impedances of the PRs are determined as [8], [9], [10];

$$f_{ii} = \frac{1}{2\pi\sqrt{L_{ai}C_{pi}}} \tag{2}$$

$$Z_{input} = \frac{jw_{ii}L_{ai}}{1 - w_{ii}^2 C_{pi}L_{ai}} \tag{3}$$

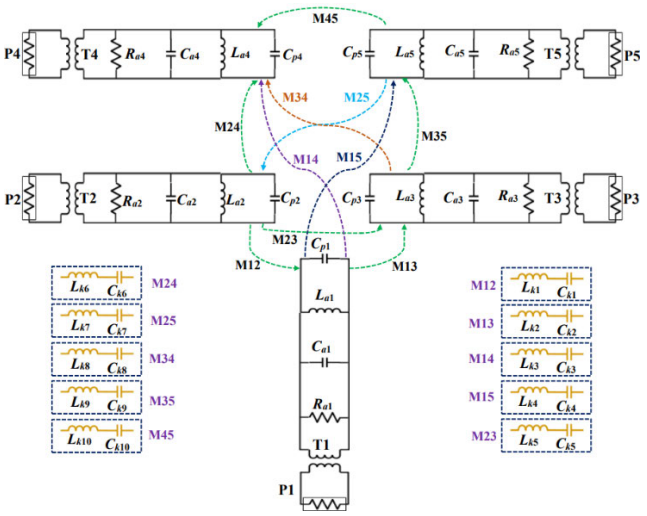

FIGURE 4. Equivalent circuit model of the proposed self-quintuplexing antenna.

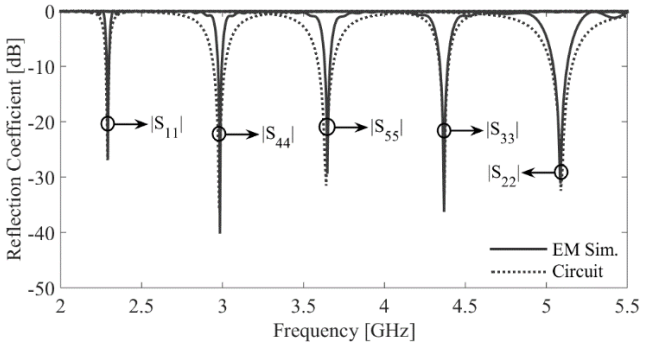

FIGURE 5. Circuit and EM simulated reflection coefficients of the proposed self-quintuplexing antenna.

TABLE 1. Component values of the equivalent circuit.

R_{a1}	L_{a1}	C_{a1}	C_{p1}	L_{k1}	C_{k1}
742	0.61	0.12	7.91	11.722	7.6549
R_{a2}	L_{a2}	C_{a2}	C_{p2}	L_{k2}	C_{k2}
281	0.33	0.02	2.96	14.851	4.507
R_{a3}	L_{a3}	C_{a3}	C_{p3}	L_{k3}	C_{k3}
457	0.31	0.04	4.27	12.71	6.6042
R_{a4}	L_{a4}	C_{a4}	C_{p4}	L_{k4}	C_{k4}
281	0.54	0.09	6.27	12.914	11.2525
R_{a5}	L_{a5}	C_{a5}	C_{p5}	L_{k5}	C_{k5}
281	0.45	0.08	4.24	12.61	6.7042
L_{k6}	C_{k6}	L_{k7}	C_{k7}	L_{k8}	C_{k8}
13.659	11.4024	12.02	14.5503	13.361	10.6529
L_{k9}	C_{k9}	L_{k10}	C_{k10}	T_1	T_2
14.255	6.2545	13.51	6.5543	0.259	0.429
T_3	T_4	T_5			
0.33	0.429	0.429			

It can be noted that the operating frequencies are controlled by the inductances L_{ai} and supplementary capacitances C_{pi}. Since the capacitances C_{pi} are varied due to the loading of PSS and TSS, the operating bands can be altered by changing the slot dimensions. Finally, the

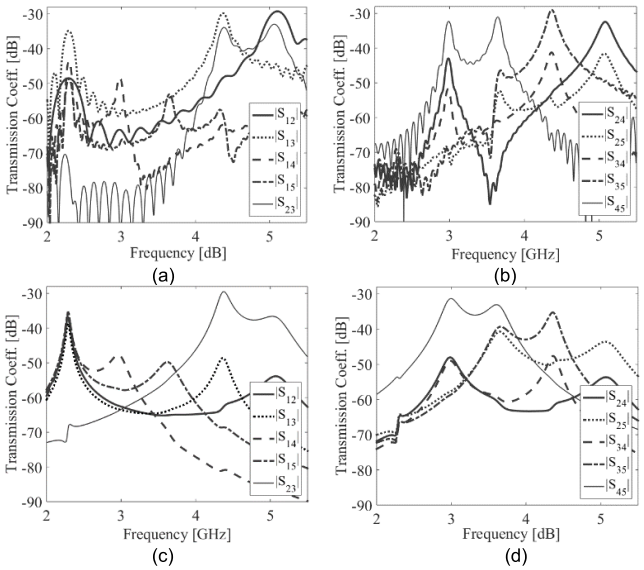

FIGURE 6. Transmission coefficients of the proposed self-quintuplexing antenna: (a, b) EM simulated and (c, d) circuit simulated.

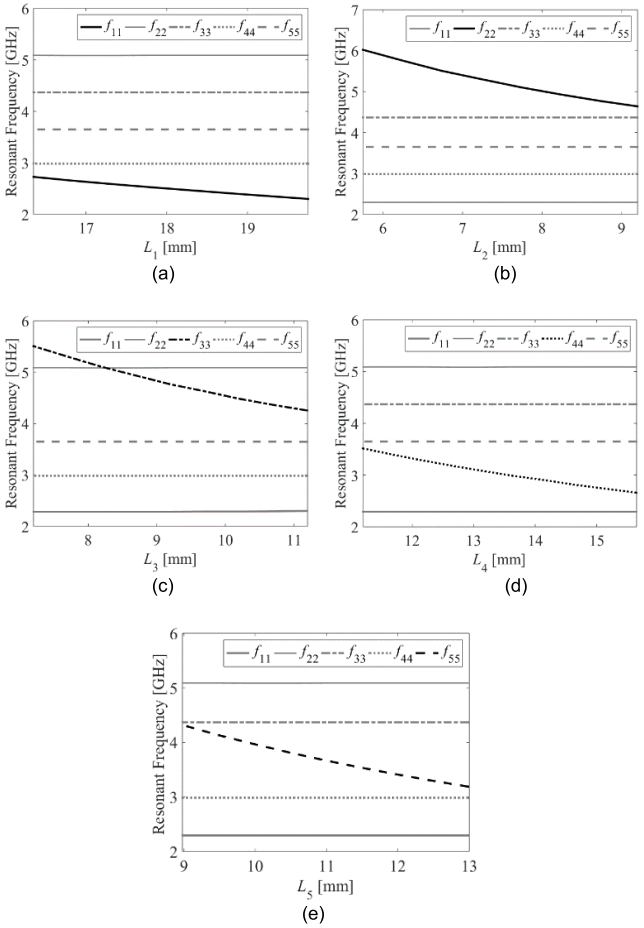

FIGURE 7. Frequency tunability of the proposed self-quintuplexing antenna associated with (a) port-1, (b) port-2, (c) port-3, (d) port-4, and (e) port-5.

equivalent model of the proposed self-quintuplexing antenna is synthesized and simulated using Keysight Advanced

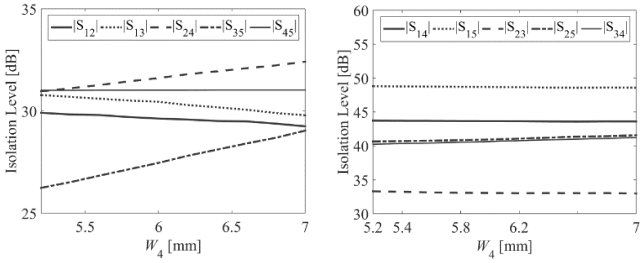

FIGURE 8. Isolation variability of the proposed self-quintuplexing antenna: (a) $|S_{12}|$, $|S_{13}|$, $|S_{24}|$, $|S_{35}|$, $|S_{45}|$, (b) $|S_{14}||$, $|S_{15}|$, $|S_{23}|$, $|S_{25}|$, $|S_{34}|$.

Design System. Table 1 presents the optimized component values of the circuit. Figure 5 shows the EM and circuit simulated reflection coefficients of the self-quintuplexing antenna with good agreement. The EM simulated transmission coefficients are presented in Figs. 6(a) and 6(b), whereas, the circuit simulated transmission coefficients are depicted in Figs. 6(c) and 6(d).

B. FREQUENCY TUNABILITY

The proposed self-quintuplexing antenna configuration offers a flexible frequency re-designability, which may accommodate several communication standards/applications such as S-band, Extended C-band, INSAT C-band, Wi-Fi, WLAN, LTE, ISM, Wi-MAX, 5G, and so on. Figure 7 shows the frequency re-designability of the presented self-quintuplexing antenna as a function of the design parameters of the PRs.

It can be noted that when one operating band is re-designed, the other four frequency bands remain unaltered and vice-versa. Also, the self-quintuplexing antenna can cover a wide frequency tuning range from 2.29 to 6.03 GHz, which supports several wireless standards. The parameters L_1, L_2, L_3, L_4, and L_5 are used to vary the operating band independently. The lower operating band f_{11} associated with port 1 can be altered from 2.29 to 2.73 GHz by changing the parameter L_1 from 16.32 to 19.82 mm as shown in Fig. 7(a). When the parameter L_2 varies from 5.734 to 9.233 mm, the operating band f_{22} related to port 2 is tuned from 4.63 to 6.03 GHz as depicted in Fig. 7(b). Referring to Fig. 7(c), the operating band f_{33} linked to port 3 can be redesigned in the range from 4.25 to 5.51 GHz by altering the parameter L_3 from 7.194 to 11.19 mm. Looking into Fig. 7(d), it is found that the operating band f_{44} associated with port 4 is tuned from 2.66 to 3.53 GHz by changing the parameter L_4 from 11.15 to 15.65 mm. Similarly, when the parameter L_5 is varied from 8.983 to 12.98 mm, the frequency band f_{55} related to port 5 can be altered from 3.19 to 4.32 GHz as shown in Fig. 7(e).

C. TRANSMISSION COEFFICIENT AND MATCHING ANALYSIS

An important performance indicator for the self-quintuplexing antenna is the transmission coefficient. The proposed self-quintuplexing antenna is configured to achieve high isolation by carefully assembling the feedlines, slots, and dimensions. Initially, the minimum isolation level at each port is found to be 20 dB due to the intrinsic properties of the configuration [8], [9]. It can be seen that port 1 is placed orthogonally to all other ports, which creates a weak cross-coupling path resulting in good isolation. The variation of isolation as a function of parameter W_4 is shown in Fig. 8. When W_4 varies from 5.2 to 7mm, it is found that the isolations $|S_{12}|$, $|S_{13}|$, $|S_{14}|$, and $|S_{15}|$ (minimum level) are better than 29.3, 29.8, 43.6, and 48.5 dB, respectively. The minimum isolation level for $|S_{23}|$, $|S_{24}|$, $|S_{25}|$, $|S_{34}|$, and $|S_{45}|$ is greater than 30.9 dB as W_4 varies from 5.2 to 7mm. Figure 8 indicates that $|S_{35}|$ can be considered to determine the minimum level for the proposed self-quintuplexing antenna, which is controlled by the parameter W_4. As we can see, the isolation $|S_{45}|$ increases from 26.2 to 29.1 by varying the parameter W_4 from 5.2 to 7mm. To ensure sufficient matching at the ports, the inline feeding technique is applied. The dimension of its inline feed controls the reflection coefficients at each port independently. Hence, the parameters a_1-a_5 (lengths) and b_1-b_5 (widths) need to be chosen carefully to achieve good matching and maintain a reflection coefficient better than –20 dB.

Considering the proposed analysis in Section II, a simple design approach can be followed to implement a self-quintuplexing antenna.

1. A SIRC with a dimension of $L_p \times W_p$ (34mm ×42mm) is chosen to support TE_{110}, TE_{120}, and TE_{210} modes operating at 3.64, 5.39, and 6.11 GHz, respectively.
2. A Pi-shaped slot and a T-shaped slot are loaded on top of the SIRC to produce five patch radiators corresponding to five microstrip feedlines.
   i. The lengths (L_1, L_2, L_3, L_4, and L_5) of the PRs are selected based on the required operating bands. For example, the lengths of the PRs for the proposed SMA are $L_1 = 0.219\lambda_g$, $L_2 = 0.086\lambda_g$, $L_3 = 0.117\lambda_g$, $L_4 = 0.15\lambda_g$, and $L_5 = 0.123\lambda_g$, where λ_g is the guided wavelength at the lower band.
   ii. For any particular operating bands, the parameters a_1-a_5 (lengths) and b_1-b_5 (widths) of feedlines need to be varied to ensure sufficient reflection coefficients.
3. The transmission coefficients of the proposed self-quintuplexing antenna can be controlled by the parameter W_4. To achieve the required isolation, the parameter W_4 needs to be tuned.
4. To achieve various wireless standards/applications with high isolation, repeat Steps 2 and 3.
5. Validate the suggested self-quintuplexing antenna through circuit simulation, EM simulation, fabrication, and measurements.

III. FABRICATION AND RESULTS DISCUSSION

To validate the proposed approach, a self-quintuplexing antenna (34 mm × 42 mm) implemented on an SIRC

TABLE 2. Performance comparison between the proposed SMA and reported SMAs.

Ref.	Freq. (GHz)	ISL (dB)	Gain (dBi)	Size (λ_g^2)	LC model	SM	Operation
[6]	1.75/1.85/1.95/2.15/2.6	NA	2.1/-1.7/1.9/3.2/4.8	0.509	No	No	Pentaband
[7]	2.31/2.57/2.91/3.11/3.35/3.61	>22	5.19/5.76/5.43/5.58/5.68/5.19	0.32	No	No	Hexa-band
[18]	8.85/10.4/11.4/12.25	>26	5.2/6/6.25/7	1.369	No	Yes	Quad-band
[19]	8.19/8.8/9.71/11	>22	5.5/6.9/7.47/7.45	0.792	No	Yes	Quad-band
[20]	5.14/5.78/6.74/7.74	>28	4.1/4.96/6.2/6.1	0.27	No	Yes	Quad-band
[21]	2.45/3.5/4.9/5.4	>29.9	3.85/5.33/5.95/5.97	0.23	Yes	Yes	Quad-band
[22]	3.5/4.9/5.4/5.8	>23.1	4.4/5.07/5.4/5.7	0.32	No	Yes	Quad-band
[23]	4.8/5.4/28/30	>20	5.4/5.2/8/8.7	0.51	Yes	Yes	Quad-band
[26]	5.33/5.76/6.31/6.86/7.34/7.8	>23.42	4.5, 4.94, 4.9, 5.12, 6.12, 6.6	0.39	No	Yes	Hexa-band
This work	**2.29/2.98/3.65/4.37/5.08**	**>29.31**	**3.59/4.55/3.91/5.70/4.92**	**0.173**	**Yes**	**Yes**	**Pentaband**

ISL: Isolation, λ_g: Guided wavelength at lower frequency band, SM: Self-multiplexing, NA: Not available

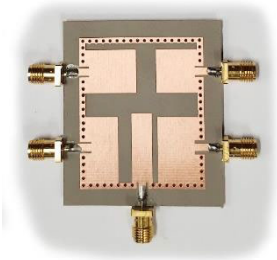

FIGURE 9. Photograph of the fabricated self-quintuplexing antenna prototype.

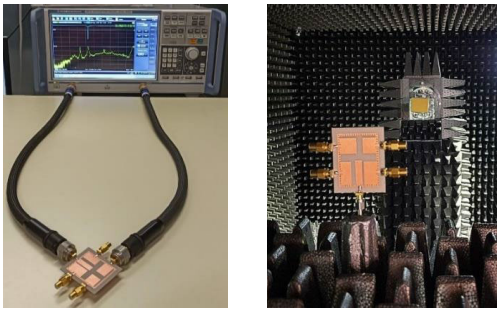

FIGURE 10. Measurement setup for the fabricated self-quintuplexing antenna: (a) reflection and transmission coefficients, (b) radiation patterns and realized gain.

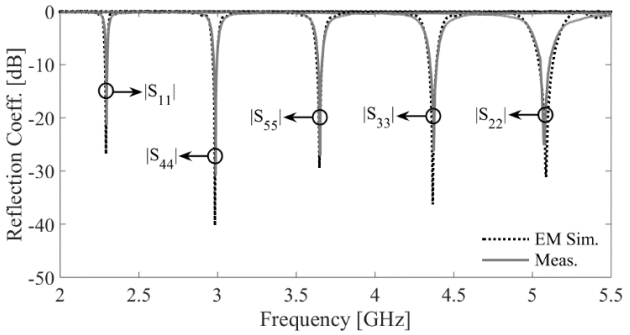

FIGURE 11. EM simulation and measured reflection coefficients of the suggested self-quintuplexing antenna.

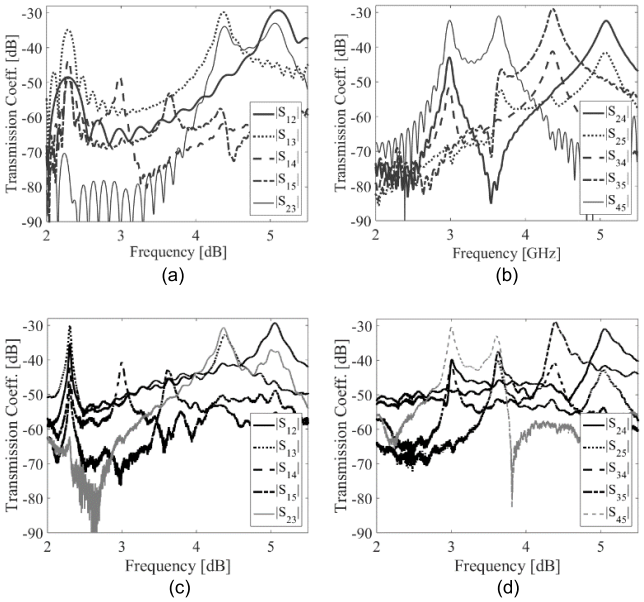

FIGURE 12. Transmission coefficients of the fabricated self-quintuplexing antenna: (a, b) EM simulated and (c, d) measurement.

resonator was fabricated and experimentally demonstrated. Figure 9 shows the photograph of the self-quintuplexing antenna prototype. The measurement setup for the *S*-parameters and radiation characteristics are depicted in Fig. 10. Figure 11 compares the EM simulated and measured reflection coefficients. The measured and EM simulated reflection coefficients ($|S_{11}|$, $|S_{22}|$, $|S_{33}|$, $|S_{44}|$, and $|S_{55}|$) are better than –21.3 dB at each band. Figure 13 shows the EM simulated and measured transmission coefficients. From Figure 12, it is obtained that the EM simulated and measured isolations ($|S_{12}|$, $|S_{13}|$, $|S_{14}|$, $|S_{15}|$, $|S_{23}|$, $|S_{24}|$, $|S_{25}|$, $|S_{34}|$, $|S_{35}|$, and $|S_{45}|$) are better than 29.3 dB. The EM simulated (experimented) 10dB matching bandwidths

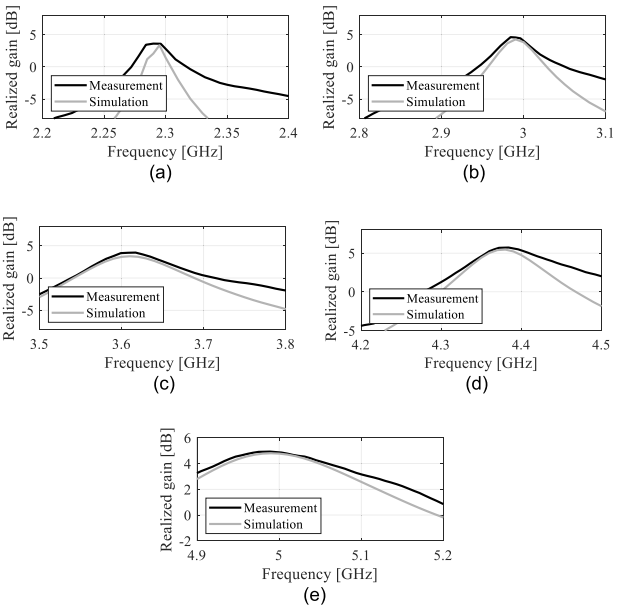

FIGURE 13. EM simulation and measured realized gains of the suggested self-quintuplexing antenna. (a) at 2.29 GHz, (b) at 2.98 GHz, (c) at 3.65 GHz, (d) at 4.37 GHz, and (e) at 5.08 GHz.

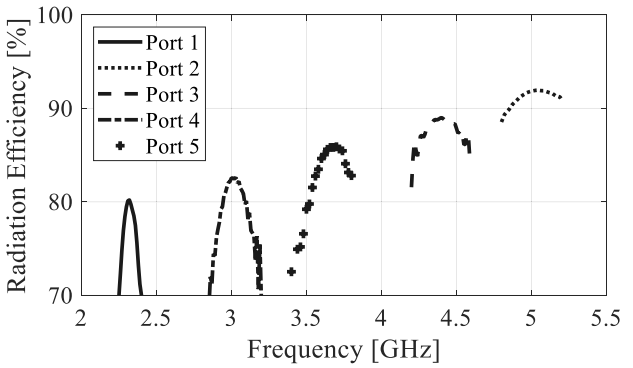

FIGURE 14. EM simulated radiation efficiency of the proposed self-quintuplexing antenna.

are 0.73% (0.41%), 0.81% (0.67%), 0.88% (0.73%), 1.19% (0.99%), and 1.73% (1.15%) at 2.29, 2.98, 3.65, 4.37, and 5.08 GHz, respectively. The proposed SQA exhibits a narrow bandwidth due to the fact that the frequency bands are highly isolated, which can be used for pinpoint wireless applications. The farfield radiation characteristics are recorded using an automatic anechoic chamber. The experiment is carried out by applying excitation to the selected port with other ports terminated using a 50Ω matched load. The EM simulated and measured realized gains are presented in Fig. 13. The EM simulated (measured) realized gains are found to be 3.34dB (3.59dB), 4.25dB (4.55dB), 3.38dB (3.91dB), 5.45dB (5.70dB) and 4.72dB (4.92dB) at 2.29, 2.98, 3.65, 4.37, and 5.08 GHz, respectively. It can be noted that the realized gain is affected due to the precision of the antenna radiating patches and the material used for it. Figure 14 shows the EM simulated radiation efficiencies from port 1 to port 5.

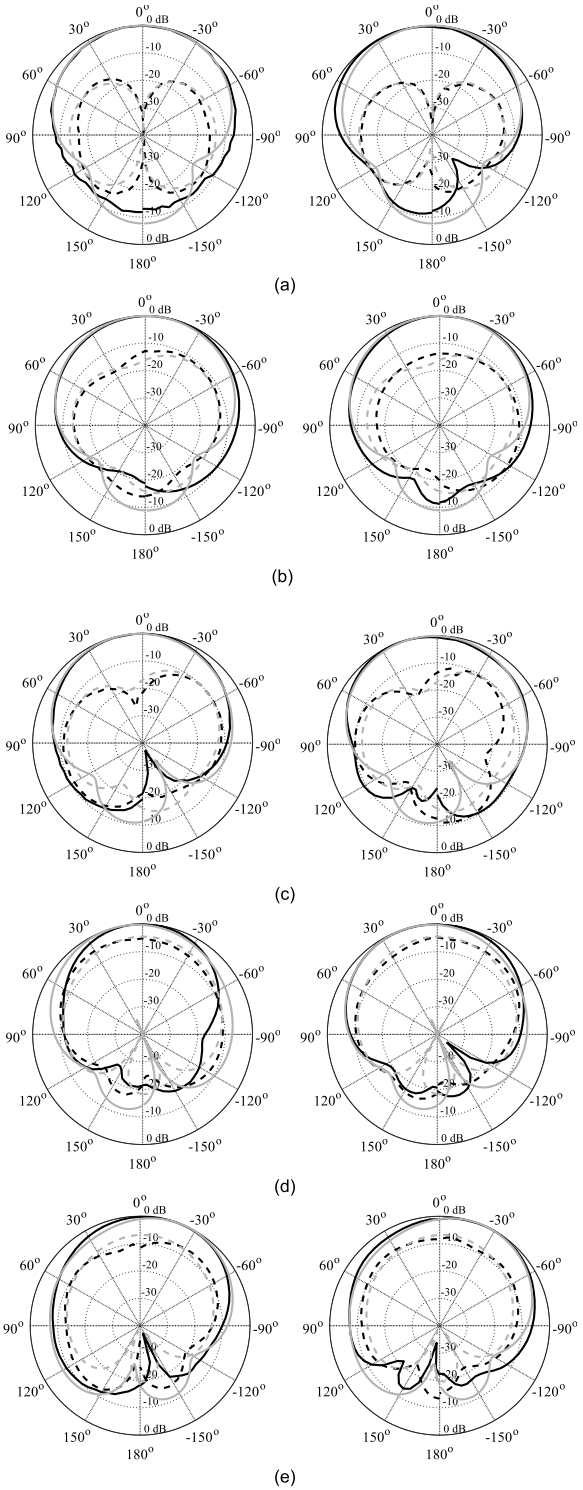

FIGURE 15. Normalized radiation pattern of the suggested self-quintuplexing antenna. (a) at 2.29 GHz, (b) at 2.98 GHz, (c) at 3.65 GHz, (d) at 4.37 GHz, and (e) at 5.08 GHz. [Simulation – grey, measurement – black); H-plane (left), E-plane (right); copol – solid, crosspol – dashed].

The recorded efficiencies are 80.19%, 82.17%, 85.72%, 88.77%, and 91.89% from port1 to port5. Figure 15 illustrates the normalized radiation patterns of the self-quintuplexing antenna prototype in the H-plane and E-plane at individual

port excitations. The self-quintuplexing antenna prototype achieves a unidirectional pattern and linear polarization. The results of the circuit, the EM simulation, and the measurements are found to be in good agreement, as expected. However, due to fabrication tolerance and connector loss, small deviations can be observed.

Table 2 compares the proposed self-quintuplexing antenna's performance indicators with the recently published self-multiplexing antennas. Comparing the proposed SQA to the existing SMAs, it is found to be extremely compact [6], [7], [18], [19], [20], [21], [22], [23], [26]. When compared to the most compact SMA of [21], the proposed SQA has a 24.8-percent smaller footprint. It also exhibits the highest isolation of 29.3 dB as compared to the reported self-multiplexing antennas [18], [19], [20], [21], [22], [23], [26], except [21]. The proposed self-quintuplexing antenna is validated using an equivalent lumped circuit. Except for [21] and [23], none of the other reported SMAs are validated by equivalent circuits, as shown in the table. The proposed self-quintuplexing antenna provides reasonable realized gain when compared to the existing self-multiplexing antennas [6], [7], [18], [19], [20], [21], [22], [23], [26]. Additionally, the proposed self-quintuplexing antenna allows a wide frequency tunability range (2.29-6.03GHz) that can accommodate most of the sub-6 GHz communication standards/ applications.

IV. CONCLUSION

This article presents a new compact self-quintuplexing antenna architecture implemented on a substrate-integrated rectangular cavity for pentaband applications. An SIRC, one Pi-shaped slot (PSS), one T-shaped slot (TSS), and five 50Ω microstrip feedlines are employed to synthesize the proposed self-quintuplexing antenna. To achieve pentaband operation with self-multiplexing characteristics, the PSS and TSS are positioned on the top surface of the SIRC resonator, resulting in five radiating patches that are excited by five 50Ω feedlines. A detailed study has been carried out to achieve tuning of individual operating bands, high isolation, and good matching at all ports. An equivalent lumped circuit has been presented to validate the proposed self-quintuplexing antenna. A simple synthesis approach has been elaborated on for the implementation of the self-quintuplexing antenna. Finally, an SIRC-based self-quintuplexing antenna operating at 2.29, 2.98, 3.65, 4.37, and 5.08 GHz has been developed and tested to verify the proposed antenna architecture. Despite its small size and pentaband operation, the self-quintuplexing antenna offers superior isolation of 29.3 dB, a frequency re-designability range of 2.29 to 6.03 GHz, and realized gains of 3.6 dB, 4.6 dB, 3.9 dB, 5.7 dB, and 4.9dB at 2.29 GHz, 2.98 GHz, 3.65 GHz, 4.37 GHz, and 5.08GHz, respectively.

REFERENCES

[1] P. Ciais, R. Staraj, G. Kossiavas, and C. Luxey, "Design of an internal quad-band antenna for mobile phones," *IEEE Microw. Wireless Compon. Lett.*, vol. 14, no. 4, pp. 148–150, Apr. 2004.

[2] D. M. Nashaat, H. A. Elsadek, and H. Ghali, "Single feed compact quad-band PIFA antenna for wireless communication applications," *IEEE Trans. Antennas Propag.*, vol. 53, no. 8, pp. 2631–2635, Aug. 2005.

[3] M. Martinez-Vazquez, O. Litschke, M. Geissler, D. Heberling, A. M. Martinez-Gonzalez, and D. Sanchez-Hernandez, "Integrated planar multiband antennas for personal communication handsets," *IEEE Trans. Antennas Propag.*, vol. 54, no. 2, pp. 384–391, Feb. 2006.

[4] K. L. Wong and C. H. Huang, "Printed loop antenna with a perpendicular feed for penta-band mobile phone application," *IEEE Trans. Antennas Propag.*, vol. 56, no. 7, pp. 2138–2141, Jul. 2008.

[5] Y. Li, Z. Zhang, Z. Feng, and M. F. Iskander, "Design of penta-band omnidirectional slot antenna with slender columnar structure," *IEEE Trans. Antennas Propag.*, vol. 62, no. 2, pp. 594–601, Feb. 2014.

[6] J. Singh, R. Stephan, and M. A. Hein, "Low-profile penta-band automotive patch antenna using horizontal stacking and corner feeding," *IEEE Access*, vol. 7, pp. 74198–74205, 2019.

[7] B. J. Niu and J. H. Tan, "Hexa-band SIW cavity antenna system integrating two antennas with high isolation," *IET Electron. Lett.*, vol. 7, pp. 74198–74205, May 2019.

[8] D. Deslandes and K. Wu, "Single-substrate integration technique of planar circuits and waveguide filters," *IEEE Trans. Microw. Theory Techn.*, vol. 51, no. 2, pp. 593–596, Feb. 2003.

[9] M. Bozzi, A. Georgiadis, and K. Wu, "Review of substrate-integrated waveguide circuits and antennas," *IET Microwave Antennas Propag.*, vol. 5, no. 8, pp. 909–920, Jun. 2011.

[10] R. K. Barik, Q. S. Cheng, S. K. K. Dash, N. C. Pradhan, and K. S. Subramanian, "Design of a compact orthogonal fed self-diplexing bowtie-ring slot antenna based on substrate integrated waveguide," *Int. J. RF Microw. Comput.-Aided Eng.*, vol. 30, no. 11, Nov. 2020, Art. no. e22422.

[11] R. K. Barik, Q. S. Cheng, S. K. K. Dash, N. C. Pradhan, and S. S. Karthikeyan, "Compact high-isolation self-diplexing antenna based on SIW for C-band applications," *J. Electromagn. Waves Appl.*, vol. 34, no. 7, pp. 960–974, May 2020.

[12] N. C. Pradhan, K. S. Subramanian, R. K. Barik, and Q. S. Cheng, "A shielded-QMSIW-based self-diplexing antenna for closely spaced bands and high isolation," *IEEE Antennas Wireless Propag. Lett.*, vol. 20, no. 12, pp. 2382–2386, Dec. 2021.

[13] R. K. Barik, S. Koziel, Q. S. Cheng, and S. Szczepanski, "Highly miniaturized self-diplexed U-shaped slot antenna based on shielded QMSIW," *IEEE Access*, vol. 9, pp. 158926–158935, 2021.

[14] A. Iqbal, I. B. Mabrouk, M. Al-Hasan, M. Nedil, and T. A. Denidni, "Wideband substrate integrated waveguide antenna for full-duplex systems," *IEEE Antennas Wireless Propag. Lett.*, vol. 21, no. 1, pp. 212–216, Jan. 2022.

[15] S. K. K. Dash, Q. S. Cheng, R. K. Barik, N. C. Pradhan, and K. S. Subramanian, "A compact triple-fed high-isolation SIW-based self-triplexing antenna," *IEEE Antennas Wireless Propag. Lett.*, vol. 19, no. 5, pp. 766–770, May 2020.

[16] S. Priya and S. Dwari, "A compact self-triplexing antenna using HMSIW cavity," *IEEE Antennas Wireless Propag. Lett.*, vol. 19, no. 5, pp. 861–865, May 2020.

[17] A. Iqbal, M. A. Selmi, L. F. Abdulrazak, O. A. Saraereh, N. K. Mallat, and A. Smida, "A compact substrate integrated waveguide cavity-backed self-triplexing antenna," *IEEE Trans. Circuits Syst. II, Exp. Briefs*, vol. 67, no. 11, pp. 2362–2366, Nov. 2020.

[18] K. Kumar, S. Priya, S. Dwari, and M. K. Mandal, "Self-quadruplexing circularly polarized SIW cavity-backed slot antennas," *IEEE Trans. Antennas Propag.*, vol. 68, no. 8, pp. 6419–6423, Aug. 2020.

[19] S. Priya, S. Dwari, K. Kumar, and M. K. Mandal, "Compact self-quadruplexing SIW cavity-backed slot antenna," *IEEE Trans. Antennas Propag.*, vol. 67, no. 10, pp. 6656–6660, Oct. 2019.

[20] S. K. K. Dash, Q. S. Cheng, and R. K. Barik, "A compact substrate integrated waveguide backed self-quadruplexing antenna for C-band communication," *Int. J. RF Microw. Comput.-Aided Eng.*, vol. 30, no. 10, Oct. 2020, Art. no. e22366.

[21] A. Iqbal, J. J. Tiang, S. K. Wong, S. W. Wong, and N. K. Mallat, "SIW cavity-backed self-quadruplexing antenna for compact RF front ends," *IEEE Antennas Wireless Propag. Lett.*, vol. 20, no. 4, pp. 562–566, Apr. 2021.

[22] A. Iqbal, M. Al-Hasan, I. B. Mabrouk, and M. Nedil, "Compact SIW-based self-quadruplexing antenna for wearable transceivers," *IEEE Antennas Wireless Propag. Lett.*, vol. 20, no. 1, pp. 118–122, Jan. 2021.

[23] H. Naseri Gheisanab, P. Pourmohammadi, A. Iqbal, A. Kishk, and T. A. Denidni, "SIW-based self-quadruplexing antenna for microwave and mm-wave frequencies," *IEEE Antennas Wireless Propag. Lett.*, vol. 21, no. 7, pp. 1482–1486, Jul. 2022, doi: 10.1109/LAWP.2022.3172007.
[24] R. K. Barik and S. Koziel, "Highly miniaturized self-quadruplexing antenna based on substrate-integrated rectangular cavity," *IEEE Antennas Wireless Propag. Lett.*, vol. 22, no. 3, pp. 482–486, Mar. 2023, doi: 10.1109/LAWP.2022.3216305.
[25] R. K. Barik and S. Koziel, "A compact self-hexaplexing antenna implemented on substrate-integrated rectangular cavity for hexa-band applications," *IEEE Trans. Circuits Syst. II, Exp. Briefs*, vol. 70, no. 2, pp. 506–510, Feb. 2023, doi: 10.1109/TCSII.2022.3211963.
[26] S. K. K. Dash, Q. S. Cheng, R. K. Barik, F. Jiang, N. C. Pradhan, and K. S. Subramanian, "A compact SIW cavity-backed self-multiplexing antenna for hexa-band operation," *IEEE Trans. Antennas Propag.*, vol. 70, no. 3, pp. 2283–2288, Mar. 2022.

RUSAN KUMAR BARIK (Member, IEEE) received the B.Tech. degree in electronics and communication engineering from the Biju Patnaik University of Technology, Rourkela, India, in 2012, and the M.Tech. degree in communication systems design and the Ph.D. degree in electronics engineering from the Indian Institute of Information Technology, India, in 2015 and 2018, respectively. From May 2018 to April 2019, he was an Assistant Professor with the Department of Electronics and Communication Engineering, Christ University, Bengaluru, India. From June 2019 to June 2021, he was a Postdoctoral Researcher with the Department of Electrical and Electronic Engineering, Southern University of Science and Technology, Shenzhen, China. He is currently a Postdoctoral Fellow with the Engineering Optimization and Modeling Center (EOMC), Department of Electrical Engineering, Reykjavik University, Iceland. His research interests include multiband microwave devices, SIW components, reconfigurable components, and multiband antennas.

SLAWOMIR KOZIEL (Fellow, IEEE) received the M.Sc. and Ph.D. degrees in electronic engineering from the Gdańsk University of Technology, Poland, in 1995 and 2000, respectively, and the M.Sc. degree in theoretical physics, the M.Sc. degree in mathematics, and the Ph.D. degree in mathematics from the University of Gdańsk, Poland, in 2000, 2002, and 2003, respectively. He is currently a Professor with the Department of Engineering, Reykjavik University, Iceland. His research interests include CAD and modeling of microwave and antenna structures, simulation-driven design, surrogate-based optimization, space mapping, circuit theory, analog signal processing, evolutionary computation, and numerical analysis.